A novel methodology to study polymodal particle size distributions produced during continuous wet granulation

Carlota Mendez Torrecillas[1,2*], Gavin W. Halbert[1,2], Dimitrios A. Lamprou[2,3*,]**

[1] EPSRC Centre for Innovative Manufacturing in Continuous Manufacturing and Crystallisation (CMAC), University of Strathclyde, Technology and Innovation Centre, 99 George Street, G1 1RD Glasgow, United Kingdom.

[2] Strathclyde Institute of Pharmacy and Biomedical Sciences (SIPBS), University of Strathclyde, 161 Cathedral Street, G4 0RE Glasgow, United Kingdom.

[3] Medway School of Pharmacy, University of Kent, Medway Campus, Anson Building, Central Avenue, Chatham Maritime, Chatham, Kent, ME4 4TB, United Kingdom.

* Corresponding Authors. E-mail address: carlota.mendez@strath.ac.uk and D.Lamprou@kent.ac.uk.

Tel.: +44(0) 163 420 2947.

** Funded by Cancer Research UK

ABSTRACT

It is important during powder granulation to obtain particles of a homogeneous size especially in critical situations such as pharmaceutical manufacture. To date, homogeneity of particle size distribution has been defined by the use of the d_{50} combined with the span of the particle size distribution, which has been found ineffective for polymodal particle size distributions. This work focuses on demonstrating the limitations of the span parameter to quantify homogeneity and proposes a novel improved metric based on the transformation of a typical particle size distribution curve into a homogeneity factor which can vary from 0 to 100%. The potential of this method as a characterisation tool has been demonstrated through its application to the production of granules using two different materials. The workspace of an 11 mm twin screw granulator was defined for two common excipients (α-lactose monohydrate and microcrystalline cellulose). Homogeneity of the obtained granules varied dramatically from 0 to 95 % in the same workspace, allowing identification of critical process parameters (e.g. feed rate, liquid/solid ratio, torque velocities). In addition it defined the operational conditions required to produce the most homogeneous product within the range 5 μm – 2.2 mm from both materials.

Keywords: Twin screw granulation; particle size distribution; homogeneity factor; quality by design; granules.

Abbreviations:

A_0	Area corresponding to the equivalent minimum homogeneity of PSD
A_{100}	Area corresponding to the equivalent maximum homogeneity of PSD
A_{PSD}	Area corresponding to the PSD
DoE	Design of experiments
d_x	Intercept x of the cumulative volume
d	Diameter
FH	Homogeneity factor
k_1	Sorting factor parameter
k_2	Sorting factor parameter
L/S	Liquid/Solid ratio
μ	Mean value
n_{interv}	Number of intervals
p	Percentage of the value of the population
PSD	Particle Size Distribution
QbD	Quality by Design
q_x	Density distribution
Q_x	Cumulative distribution
s	Sorting factor
VMD	Volume mean diameter

61	TSG	Twin-Screw Granulator
62	w(d)	Weight distribution
63	w_{PSD}	Weight distribution corresponding to the particle size distribution
64	w_0	Weight distribution corresponding to the equivalent minimum homogeneity of PSD
65	w_{100}	Weight distribution corresponding to the equivalent maximum homogeneity of PSD
66	xm	Particle size
67	xm_0	Particle size of the first value
68	xm_{max}	Particle size of the maximum peak
69		

1. INTRODUCTION

Wet granulation is a common industrial unit operation in the pharmaceutical industry for particle size enlargement. Although this operation has been traditionally performed in batch, it could be effectively achieved in a continuous mode using a Twin-Screw Granulator (TSG). The key advantages of this technology over batch granulation are shorter residence times, greater flexibility in granule properties and the ability to vary the required throughput. The understanding of wet granulation has achieved notable advances in the past twenty-five years, since the macroscopic research of granulation was replaced by a microscopic study of the variables ((Ennis and Litster, 1997; Ennis, 1991; Parikh, 2005)).

In contrast to batch equipment traditionally used in wet granulation, TSG has been applied by the pharmaceutical industry as a useful continuous operation granulation technique (Keleb et al., 2002; Van Melkebeke et al., 2008), which due to the flexibility offered by the equipment is easier to design and scale up. Multiple working environments are enabled by the possibility of changing different sections of the screw assembly, feed port locations, different segment geometry's or the option of working with a wide range of conditions such as feed rate or liquid/solid ratio (Dhenge et al., 2011; Djuric and Kleinebudde, 2008; Vercruysse et al., 2012). Vercruysse (Vercruysse et al., 2013), for example confirmed the successful production of granules by TSG processes within the specifications defined for the equivalent batch fluid bed granulation process. Furthermore, this system was able to manufacture simplified formulations containing high drug loads of up to 90% (Meier et al., 2015). On the contrary, other cases where there is a lack of specific tools to study the operational parameters were driven to situations where the implementation of TSG was not justified compared to batch systems (Lee et al., 2013).

One of the main explanations is that the variation in the conditions produces many different Particle Size Distributions (PSD) for which the curves differ from the desired unimodal shape (Yu et al., 2014) achieved during standard batch granulation processes. The appearance of polymodal distributions is especially prevalent during research into the effects that the parameters have on granule properties. Particle size distributions vary from unimodal to polymodal depending on the analysed value or position of the variable. That is especially remarkable, in the different studies about the influence of the main parameters such as liquid/solid ratio (L/S) or screw elements (Dhenge et al., 2012; El Hagrasy et al., 2013; Sayin et al., 2015).

The evaluation of the granulation process requires knowledge of the variance of the granules' properties as function of the process parameters, and, the establishment of the variation using general terms such as volume, strength, and friability. The study of these terms gives important information allowing process control, as well as establishment of the acceptable limits of the working conditions. However, although terms such as friability or flowability can be expressed as a single value, particle size distribution is frequently expressed as a curve, which does not allow its direct examination as a quality attribute or a process control variable. A quality attribute should be within an appropriate limit, range, or distribution to ensure the desired product quality (ICH Q8 (R2), 2009).

The separation of a particulate sample into discrete size classes has been traditionally performed representing the type of quantity in the abscissa and the measure of the quantity in the ordinate. The measurement of the quantity is made through the relative amount of particles measured within a specific size interval and it is called density distribution (q_x). This term is the first derivative of the cumulative distribution (Q_x) against particle size (Leschonski, 1984). The subscript x represents the type of quantity where the possible types are number, length, area, volume or mass. In pharmaceutical sciences, the type of quantity chosen is frequently the

118 volume, due to the importance of the relationship between drug delivery and volume (Müllertz
119 et al., 2016).

120 Frequently, the volume particle size distributions are characterised by d_{10},d_{50} and d_{90} which are
121 calculated through the intercepts for 10, 50 and 90 % of the cumulative volume (ISO, 2014).
122 These terms can be gathered if they are transformed to the span $((d_{90} - d_{10})/d_{50})$ (Chitu et al.,
123 2011; El Hagrasy et al., 2013), with particle size distributions considered more homogeneous
124 the closer this value is to zero. This analysis is only acceptable when the particle size
125 distribution is lognormal, but will introduce a considerable error when the distributions show
126 more than one peak and the peaks are located around the mean diameter. For instance, Figure
127 1 shows two particle size distributions which have two different shapes but very close span
128 values. The first shape (Figure 1a) could be considered to be a common lognormal distribution
129 where all the values are around the main peak. However, the second shape (Figure 1b) displays
130 three peaks of different population densities which indicates that three main types of granules
131 exist in the sample. Nevertheless, the difference between spans of those distributions is less
132 than 2%, and therefore both distributions would be comparable in terms of homogeneity even
133 if they are clearly different in the number of peaks.

134 In sedimentology an alternative method has been applied to transform the normal distribution
135 for unimodal and bimodal distributions known as the hyperbolic tangent technique (tanh
136 method), which has been used traditionally for dealing with travelling waves and to study
137 evolution equations (Malfliet, 2004). It was successfully applied by Passe (Passe, 1997) in
138 order to transform a grain distribution into a mathematical expression. Due to the fact that the
139 graphical result of the integral of a normal distribution presents an analogous shape to the
140 hyperbolic tangent function; the cumulative expression can be mathematically described by
141 Eq. 1.

$$w(d) = \frac{p}{2} - \left(\frac{p}{2}\right) * \tanh(\log(\mu) - \log(d) * s) \quad \text{Eq. 1}$$

Where w is the weight, μ is the mean value of the particle size, d is the variable particle size, p is the value of the population of the different peaks in percentage which is equal to 100% for unimodal distributions and s is a sorting factor which is given as $1/(\log d_{75} - \log d_{25})$ (Passe, 1997).

This technique for transforming curves into mathematical expressions can be used as an effective way to smooth distribution curves due to the variation of the slope depending on the number of peaks. For example, three different particle size distributions have been transformed through this method in Figure 2 representing the weight against the logarithm of the particle size. The first PSD (Figure 2a) can be considered as a mono-modal distribution and its equivalent weight distribution is a straight line which slopes up at the greatest rate. The second PSD (Figure 2b) corresponds to a bimodal distribution and its weight distribution shows an important decrease of the slope of the curve compared to Figure 2a. The third PSD (Figure 2c) represents a polymodal distribution with three clear peaks in which the slope of the corresponding weight distribution curve has decreased even more dramatically with respect to Figure 2a. Therefore, from Figure 2 it can be concluded that the decreasing slope of the curves represents the decrease in homogeneity of distribution as well as the increase in the number of peaks of the distribution.

The direct relationship between the slope of the weight distribution curve and the shape of the particle size distribution shows an enormous potential as a characterisation tool. The area under the resultant curve can be calculated through integration and it will be proportional to the slope of the curve. The homogeneity can be measured through this method and transformed into a percentage, unimodal PSDs will be associated with larger areas and greater homogeneity percentages.

Transforming PSDs into a homogeneity factor (FH) allows the analysis of the influence of operational parameters on the system. In addition, workspaces can be created and the system can be easily optimised after obtaining the regions where the production of granules is homogeneous.

Further potential advantages of homogeneity values calculated from particle size distributions are related to its potential to be used as a characterisation tool for Quality by Design (QbD) which is recommended for adoption by the pharmaceutical industry (Seem et al., 2015). This approach ought to be accomplished with a systematic scientific risk-based methodology, therefore a tool for characterising granule homogeneity would help to provide a greater understanding of the underlying process mechanisms. In addition, it will improve the control during granule manufacture as well as being a useful complement to other granule properties such as flowability or strength in the optimisation of tabletting and associated processes. Besides, the possibility of defining a desired diameter operating point and controlling the homogeneity around that point allows identification of when the process is within product specifications. This advantage could be used in the comparison of different batches and technologies both research and industrial scale.

Due to the possible advantages of quantifying a PSD's homogeneity with a single numerical parameter, the aims of this study were to propose a methodology capable of achieving this. The method developed can transform any PSD into a weight distribution through the hyperbolic tangent method and calculate a homogeneity percentage. Furthermore, this method was mathematically validated through the study of the response to simulated scenarios of particle size distributions and empirically demonstrated through the application to two different materials (α-Lactose monohydrate and microcrystalline cellulose) and its potential as characterisation tool was assessed by determining the most critical process parameters for both systems.

2. MATERIALS AND METHODS

2.1. Materials

α-Lactose monohydrate (PubChem CID: 24896349) with 99% total lactose basis (GC) (Sigma-Aldrich Company Ltd., Dorset, England) and microcrystalline cellulose (PubChem CID: :16211032) with average particle size 50 µm (Fisher Scientific UK Ltd, Loughborough, Leicestershire, United Kingdom) were used as excipients to validate the method. Distilled water (EMD Millipore™ Pure Water Reservoirs, Millipore SAS, Mosheim, France) was added as granulation liquid.

2.2 Granulation experiments

In order to produce granules, a Thermofisher Pharma 11mm Twin Screw Granulator (Process 11, 40:1 L/D, Thermo Fisher Scientific, Karlsruhe, Germany) operating within the range of 50-125 rpm in combination with a gravimetric feeder (Brabender Gravimetric feeder DDW-MT, Brabender Technologie Gmbh & Co. Kg Duisburg, Germany) was employed to feed excipients at a rate of 0.05-0.35 kg h^{-1}. Distilled water was fed to the system through a syringe pump (Harvard Syringe Pump, Harvard Apparatus UK, Cambridge, UK) in order to produce liquid/solid ratios from 0.05 to 0.2 for α-Lactose monohydrate, and 1 to 1.8 for microcrystalline cellulose. The upper and lower limits of granule production ratios were chosen since below the lower limit, the product obtained at these torque velocities was a powder and above the upper limit the product was a wet mass. The design of experiments and following analysis was done through the use of the commercial software Modde 10.1. The chosen model design used to select the experimental setup and to study the relationship between variables was an Onion D-Optimal model with two layers which was fitted afterwards with PLS-2PLS regression analysis (MKS Data Analytics Solutions, Malmö, Sweden). Figure 3 displays the design of experiments for both materials: α-Lactose monohydrate (Figure 3a) and for microcrystalline cellulose

(Figure 3b). The screw configuration used was 27 conveying elements for each sheet, chosen in order to minimise the impact that the different screw elements could have on the granules (Seem et al., 2015).

2.3 Offline granule size analysis

The analysis of the granule size distribution was performed using the QICPIC/RODOS L with vibratory feeder VIBRI/L (Sympatec GmbH System-Partikel-Technik, Clausthal-Zellerfeld, Germany).

All the particle size distributions obtained were produced at 0.5 bar of primary pressure to avoid breakage of the granules during the analysis (MacLeod and Muller, 2012). The disperser conditions were optimised for each set of granules to obtain the optimal optical concentration. All the particle size distributions were plotted in logarithmic volume against the particle size. The volumetric mean diameter (VMD) determined by the system was chosen as mean diameter, and is been calculated based in the arithmetic mean value.

2.4 Quantification of homogeneity method

To quantify homogeneity PSD curves are smoothed through the hyperbolic tangent method in order to adapt the data to the mathematical expression in Eq. 2 based in the equation used by Passe. (Passe, 1997).

$$w(xm) = \sum_{0}^{i=total\ peaks} \left(\frac{p_i}{2} - \frac{p_i}{2} * \tanh(\log(\mu_i) - \log(xm) * s_i\right) \quad \text{Eq. 2}$$

Where the subindex i represents the peak number for appearance order, p_i is the value of the population of the peak in percentage, μ_i is the mean value of the particle size for the peak width,

xm is the size of the particles included in the width of the peak, and s_i is a sorting factor defined in Eq 3.

This mathematical expression depends on the total number of peaks and a specific expression needs to be developed for each peak. The peaks are local maxima of the particle size distribution. The local maximum is located as the data point which is larger than its two neighbouring points, in those cases that the top of the peak is flat, the point considered is the first to appear (The MathWorks Inc, 2013). After locating the peaks, their amplitude was calculated by means of the integral of the curve formed by the peak.

The sorting factors for each PSD curve are calculated using Eq 3 were d_{25} and d_{75} are the diameter corresponding to the 25% and 75% population weight of each peak. The sorting factor was adapted from the method presented by Passe (Passe, 1997) through the introduction of the terms k_1 and k_2 which were developed in house for the range 5 μm – 2.2 mm. The term k_1 weights the difference between the peak corresponding to maximum value in the density distribution and the volumetric mean diameter of the particles (Eq. 4). Frequently, the limits of the ranges of particles sizes distribution are proportional to the size of particle and those could be different depending on the choice of nest of sieves or the measuring range of the analytical system. To avoid the effect of these possible discrepancies between the different methods, the distribution will be normalised when one considers that it is composed of ten identical intervals. The difference between the maximum peak and the mean diameter will be measured through the number of intervals between them (Eq. 5).

$$s_i = k_1 * \frac{p_i}{\log(d_{75}) - \log(d_{25})} \quad \text{Eq. 3}$$

$$k_1 = \exp\left(-\left(\frac{xm_{\max\ peak} - d}{k_2}\right)\right) \quad \text{Eq.4}$$

$$k_2 = 10 * \frac{xm_{last} - xm_0}{n_{interval}} \quad \text{Eq. 5}$$

After the particle size distributions have been smoothed, it is required to achieve the maximum homogeneity possible, e.g. the distribution obtained when all the granules would have the same diameter and that coincides with the mean diameter. The maximum homogeneity corresponds to the best case scenario of a unimodal distribution where the first value which would appear would be unique and it would produce a single peak. After this equivalent perfect particle size distribution has been calculated, it is possible to calculate the weight distribution for that case.

The lower limits corresponding to zero homogeneity would be represented by the curves produced when all the sizes have the same weight inside the distribution. As in the case of the perfect distribution, the PSD needs to be transformed to worst case scenario, allowing the weight distribution to be calculated. Figure 4 displays the situation where both maximum and minimum cases have been transformed into their equivalent distribution. The differences in the rise of both curves allow to distinguish clearly between them as the curve corresponding to 100% homogeneity has a slope 15 times greater than the curve corresponding to 0%.

Once the upper and lower limits have been determined, it is possible to calculate the homogeneity for any particle size distribution by calculating the area under the curve corresponding to the PSD and its equivalent best (100% homogeneity) and worst (0% homogeneity) cases. Figure 5 displays the three areas in different colours. The area corresponding to 100% homogeneity would be comprised between the solid and dotted black lines with the PSD area shaded in yellow. Since the particle size distribution is given in intervals, it was chosen to obtain the area under curve through the trapezoidal rule (Treiman, 2014).

The homogeneity factor can then be calculated as percentage using Eq. 6.

$$FH\ (\%) = 100 - \ 100 * \left(\frac{\int w_{PSD}(\log(xm))dx - \int w_0(\log(xm))dx}{\int w_{100}(\log(xm))dx - \int w_{PSD}(\log(xm))dx}\right) \quad \rightarrow$$

$$FH\ (\%) = 100 - \frac{A_{PSD} - A_0}{A_{100} - A_0} * 100 \qquad \text{Eq. 6}$$

A summary of the methodology can be found in a flowchart in Figure 6.

All the data and analysis processing were performed using the commercial software package Matlab (can be found under the supplemental information) and Statistics Toolbox R2014a (The MathWorks, Inc., Natick, Massachusetts, United States).

2.5 Contour profiles

The results and the effects of the different variables will be presented as contour plots, which are able to show multidimensional interactions between the input variables and process parameters. The contour profiles are a recommended tool to identify the design space of a full workspace (ICH Q8 (R2), 2009). These profiles are built identifying which combinations of the selected parameters produce the same result on the chosen variable and identifying them with the same contour.

In this case, for each material analysed four different profiles were produced. Two for each quality attribute (homogeneity factor and volumetric mean diameter) at two different ranges of torque velocity (50-87.5 rpm and 87.5-125 rpm). The chosen process parameters were the mass feed rate of the solid and the liquid/solid ratio (L/S) which is defined as the relationship between the mass feed rate of the solid and the liquid. A schematic of the Design of experiments (DoE) can be found in Figure 3.

3. RESULTS and DISCUSSION

3.1 Verification of the methodology

According to Eq.2, the homogeneity factor is sensitive to changes in factors such as the number of the peaks or the width of the distribution. The methodology was verified through comparing the response of different simulated distributions with volumetric mean diameter equal to 1000 μm.

In the first case (Figure 7a), the effect of modification of the distribution shape was studied through the increase of the standard deviation of the distributions from 0.1 to 0.25. The increase of the standard deviation in a unimodal distribution produced a direct change in the width of the distribution, and as Figure 7a shows that affects directly in the FH. Additionally, Figure 7e shows the trend for greater increases in the standard deviation.

In the second case, the effect of introducing a peak (Figure 7b) and three peaks (Figure 7c) can be studied in two different widths. The effect of introducing a new peak produced a fall in the homogeneity as the initial homogeneity is considerably lower than that corresponding to a single peak for both widths. Figure 7f shows the effect of the increase of number of peaks from a unimodal distribution with a standard deviation of 0.25 to five peaks in the same width. As it can see, the addition of peaks produce dramatic falls in the homogeneity.

In the last case (Figure d and g), the distance between peaks was studied. The FH is sensitive to the introduction and distance between peaks as the two peaks are far apart showed a lesser degree of homogeneity than when they were closer (Figure 7d).

Other factors which will affect the FH are the distance between the volumetric mean diameter and the main peak. Those cases in which the diameter is situated around the main peak will have greater homogeneity than those in which the diameter is more distant.

To illustrate this the analysis was applied to three different real samples (see Figure 8) where the homogeneity varied from 0 to 75%. In the first case (Figure 8a) homogeneity is negligible (0%), since the sample has three main classes of particles with two of them with similar intensity in the density curve. However, the volumetric mean diameter (VMD) is skewed by a greater percentage of fines which reduces dramatically the homogeneity. In the second case (Figure 8b), there are again three classes of particles but even if the width is bigger than in the other cases, the mean diameter is placed closer to the middle of the three peaks. Therefore, the sample is more homogeneous than previous case as the VMD is closer to the biggest peak (38.3%). In the third case (Figure 8c), the PSD shape is more similar to a lognormal distribution suggesting the product is more homogeneous (74.8%). In this example, most of the particles have the same diameter. This can be observed from the PSD as well as from the photographs (Figures 8a-c).

3.2 Application of the methodology

The methodology was applied to granules produced in the TSG with two different excipients commonly used in pharmaceutical processing, α-Lactose monohydrate and microcrystalline cellulose, in a wide range of conditions. The results allow understanding of the influence different parameters have on the product homogeneity.

The results obtained were presented through contour profiles (Figure 9 and 10). These types of graphs are really effective for summarising entire workspaces. On one hand, once the region of the desired diameter has been located, the operational conditions which produce the most homogeneous granules for that exact diameter can be easily determined.. On the other hand, the contour profiles allow examination of the effects that operational parameters have over the chosen variables. For instance, on a workspace created by changing the value of two parameters, it is possible to identify if the response of the variable has been controlled by only

one or both operational parameters. That effect would be noticed since the variable would change linearly and proportionally to the axis of the most relevant parameter. In those cases, that the system would vary depending of both parameters, the response of the variable could adopt different shapes such as slanting or curved lines.

As it can be observed in Figure 9, granules of α-Lactose monohydrate were produced using different conditions of liquid/solid (L/S), feed rate and torque velocity. The results show that at low torque velocities (Figures 9a and b), the diameter shows higher dependence on the feed rate than the L/S ratio. The larger granules are produced when the feed rate is reaching the maximum with a high ratio of homogeneity and it can be observed that homogeneity of the process is more influenced by the feed rate than by the L/S ratio.

At high torque velocities (Figures 9c and d) homogeneity decreases with respect to the low torque velocities. The maximum homogeneity for this case does not reach 70% and the greater diameter which homogeneity over 50 % is not bigger than 1600 μm. On the contrary to low torque velocities, homogeneity and diameter displayed a nearly equal dependence for both parameters: L/S and feed rate. The production of homogeneous granules is achieved when the feed rate and the L/S ratio are at middle point conditions of the range of operation. At the same time, the diameter increases proportionally to both. For instance, Figure 9d would give a range of operational conditions which produce a target granule diameter. The most adequate parameters to produce a homogeneous product would be found in the Figure 9c, corresponding to a proportion to L/S ratio to Feed rate close to 1.3 to 1.

Besides, comparing low torque velocities (Figures 9 a and b) with high torque velocities (Figures c and d), it can be concluded that for α-Lactose monohydrate the degree of filling of the screw is a very important factor. At low torques velocities, high degrees of filling are achieved and the system is more dependant of the amount of powder introduced. At higher

velocities, the degree of filling is considerably lower and the system requires a balance between both parameters to obtain a desirable product.

Granules of microcrystalline cellulose were produced in an identical manner and the results are presented in Figure 10. Unlike the previous example, the diameter profiles (Figures 10 b and d) show nearly equal dependence to both parameters L/S ratio and feed rate in both cases of torque velocity. However, there is a great difference between the diameters of the particles resulting in granules up to seven times larger than when the system is operated at low torque velocities.

On the contrary, homogeneity (Figures 10 a and c) shows greater dependence to the L/S ratio than to feed rate. Furthermore, at L/S ratios above 1.52, the product reaches homogeneities of over 50% in both cases. Comparing the differences between contours profiles at low and high torque velocities indicates that the degree of filling is one of the main factors to take into account in the cellulose microcrystalline example as the low torque velocities show more disturbances than the high torque velocities.

In addition to the study individual effects, a comparison between Figures 9 and 10 permits appreciation of the strong behavioural differences between both materials. The growth of both microcrystalline cellulose and α-Lactose monohydrate granules depends dramatically on the L/S ratio, feed rate and torque velocities. Microcrystalline cellulose displays a dramatically greater dependence to the amount of liquid present in the system than α-Lactose monohydrate. This effect agrees with the molecular differences of both materials and the capability of microcrystalline cellulose to physically hold higher amounts of water than α-Lactose monohydrate (Fielden et al., 1988). In addition, these results agree with the outcomes reported by Dhenge et al., where larger granules were also found at the higher L/S ratios (Barrasso et al., 2013; Dhenge et al., 2010). Furthermore, it was described that an increase in powder feed

rates reduced the number of peaks in the PSDs (Dhenge et al., 2011), which corresponds with the increase of homogeneity reported in the case of low torque velocities for both materials. Although the most homogeneous product for the studied range were obtained, not all the experimental results can be entirely compared with those presented in the literature due to the crucial role of the screw elements configuration. However, this and published studies all present similar responses to the modifications of the operational parameters as well as similar range of diameters of granules which indicates the validity of this proposed analysis method.

Furthermore, this analysis identified the degree of filling as a limiting operational parameter for both materials which will require to be measured quantitatively in further studies of the equipment.

4. CONCLUSIONS

A new methodology for measuring homogeneity of particle size distribution was introduced and validated through its use in two different cases of granulation. The method is able to calculate the homogeneity of PSDs with different shapes allowing easy numerical comparison. The method responded to different modifications such as the addition of peaks, increments on the variation of the distribution or discrepancies between the main diameter and main particle size class. The improvement of this method with respect to the traditional measures such as span was demonstrated through the comparison of PSD curves with different shape but similar span. In addition, the potential of the quantification of homogeneity was demonstrated through the application to simple liquid granulation with two different excipients. In both cases, it was demonstrated that knowing the diameter individually does not give enough information for the ideal conditions to operate or which operational parameters have more influence on the process. Therefore, using homogeneity as a quantified quality attribute leads to a better understanding of powder technology and its possible implementation as characterisation tool in the design and control of wet granulation systems. Future work will involve the study of this tool as process control variable through a sensitivity analysis in an inline process analytical technique.

Acknowledgements

The authors would like to thank EPSRC and the Doctoral Training Centre in Continuous Manufacturing and Crystallisation (CMAC) for funding this work. The authors would also like to thank Dr Javier Cardona for corrections in the MatLab code.

Figure 1. Unimodal (a) and polymodal (b) particle size and cumulative distributions.

Figure 2. Unimodal (a) and polymodal (b, c) particle size distributions transformed to the equivalent weight distributions (d).

Figure 3. Design of experiments for α-Lactose monohydrate (a) and cellulose microcrystalline (b).

Figure 4. Equivalent particle size distributions (a) transformed to weight distributions (b).

Figure 5. Area under the weight distributions.

Figure 6. Methodology flowchart.

Figure 7. Study of the effect of the deviations produced by a change in the amplitude of the peak (a, e), increase of the number of peaks (b, c, f) and distance between the peaks (d, g).

Figure 8. Granules with homogeneity 0% (a), 38.3% (b) and 74.8% (c).

Figure 9. Homogeneity and diameter contour profiles for α-Lactose monohydrate: low torque velocities (a, b) and high torque velocities (c, d).

Figure 10. Homogeneity and diameter contour profiles for cellulose microcrystalline: low torque velocities (a, b) and high torque velocities (c, d).

448 **References**

449 Barrasso, D., Walia, S., Ramachandran, R., 2013. Multi-component population balance
450 modeling of continuous granulation processes: a parametric study and comparison with
451 experimental trends. Powder Technology 241, 85-97.
452 Chitu, T.M., Oulahna, D., Hemati, M., 2011. Wet granulation in laboratory-scale high shear
453 mixers: effect of chopper presence, design and impeller speed. Powder Technology 206, 34-
454 43.
455 Dhenge, R.M., Cartwright, J.J., Doughty, D.G., Hounslow, M.J., Salman, A.D., 2011. Twin
456 screw wet granulation: Effect of powder feed rate. Advanced Powder Technology 22, 162-166.
457 Dhenge, R.M., Cartwright, J.J., Hounslow, M.J., Salman, A.D., 2012. Twin screw wet
458 granulation: Effects of properties of granulation liquid. Powder Technology 229, 126-136.
459 Dhenge, R.M., Fyles, R.S., Cartwright, J.J., Doughty, D.G., Hounslow, M.J., Salman, A.D.,
460 2010. Twin screw wet granulation: Granule properties. Chemical Engineering Journal 164,
461 322-329.
462 Djuric, D., Kleinebudde, P., 2008. Impact of screw elements on continuous granulation with a
463 twin-screw extruder. Journal of pharmaceutical sciences 97, 4934-4942.
464 El Hagrasy, A., Hennenkamp, J., Burke, M., Cartwright, J., Litster, J., 2013. Twin screw wet
465 granulation: influence of formulation parameters on granule properties and growth behavior.
466 Powder Technology 238, 108-115.
467 Ennis, B., Litster, J., 1997. Particle size enlargement. Perry's Chemical Engineers' Handbook,
468 7th edn, McGraw-Hill, New York, 20-56.
469 Ennis, B.J., 1991. On the mechanics of granulation. UMI.
470 Fielden, K., Newton, J.M., O'BRIEN, P., Rowe, R.C., 1988. Thermal studies on the interaction
471 of water and microcrystalline cellulose. Journal of pharmacy and pharmacology 40, 674-678.
472 ICH Q8 (R2), 2009. ICH HARMONISED TRIPARTITE GUIDELINE, Step 4 Version.
473 ISO, 2014. Represenation of results of particle size analysis Part 2: Calculation of average
474 particle sizes/ diameters and moments from particle size distributions, BS ISO 9276-2:2014.
475 Bristish Standard Institution.
476 Keleb, E., Vermeire, A., Vervaet, C., Remon, J.P., 2002. Continuous twin screw extrusion for
477 the wet granulation of lactose. International journal of pharmaceutics 239, 69-80.
478 Lee, K.T., Ingram, A., Rowson, N.A., 2013. Comparison of granule properties produced using
479 Twin Screw Extruder and High Shear Mixer: A step towards understanding the mechanism of
480 twin screw wet granulation. Powder Technology 238, 91-98.

481 Leschonski, K., 1984. Representation and evaluation of particle size analysis data. Particle &
482 Particle Systems Characterization 1, 89-95.
483 MacLeod, C.S., Muller, F.L., 2012. On the fracture of pharmaceutical needle-shaped crystals
484 during pressure filtration: case studies and mechanistic understanding. Organic Process
485 Research & Development 16, 425-434.
486 Malfliet, W., 2004. The tanh method: a tool for solving certain classes of nonlinear evolution
487 and wave equations. Journal of computational and applied mathematics 164, 529-541.
488 Meier, R., Thommes, M., Rasenack, N., Krumme, M., Moll, K.P., Kleinebudde, P., 2015.
489 Simplified formulations with high drug loads for continuous twin-screw granulation.
490 International Journal of Pharmaceutics 496, 12-23.
491 Müllertz, A., Perrie, Y., Rades, T., 2016. Analytical Techniques in the Pharmaceutical
492 Sciences. Advances in delivery science and technology.
493 Parikh, D.M., 2005. Handbook of pharmaceutical granulation technology. CRC Press.
494 Passe, T., 1997. Grain size distribution expressed as tanh-functions. Sedimentology 44, 1011-
495 1014.
496 Sayin, R., Martinez-Marcos, L., Osorio, J.G., Cruise, P., Jones, I., Halbert, G.W., Lamprou,
497 D.A., Litster, J.D., 2015. Investigation of an 11 mm diameter twin screw granulator: Screw
498 element performance and in-line monitoring via image analysis. International Journal of
499 Pharmaceutics 496, 24-32.
500 Seem, T.C., Rowson, N.A., Ingram, A., Huang, Z., Yu, S., de Matas, M., Gabbott, I., Reynolds,
501 G.K., 2015. Twin screw granulation—A literature review. Powder Technology 276, 89-102.
502 The MathWorks Inc, 2013. Release, Matlab. Inc., Natick, Massachusetts, United States 488.
503 Treiman, J.S., 2014. Calculus with Vectors. Springer.
504 Van Melkebeke, B., Vervaet, C., Remon, J.P., 2008. Validation of a continuous granulation
505 process using a twin-screw extruder. International journal of pharmaceutics 356, 224-230.
506 Vercruysse, J., Córdoba Díaz, D., Peeters, E., Fonteyne, M., Delaet, U., Van Assche, I., De
507 Beer, T., Remon, J.P., Vervaet, C., 2012. Continuous twin screw granulation: Influence of
508 process variables on granule and tablet quality. European Journal of Pharmaceutics and
509 Biopharmaceutics 82, 205-211.
510 Vercruysse, J., Delaet, U., Van Assche, I., Cappuyns, P., Arata, F., Caporicci, G., De Beer, T.,
511 Remon, J.P., Vervaet, C., 2013. Stability and repeatability of a continuous twin screw
512 granulation and drying system. European Journal of Pharmaceutics and Biopharmaceutics 85,
513 1031-1038.

514 Yu, S., Reynolds, G.K., Huang, Z., de Matas, M., Salman, A.D., 2014. Granulation of
515 increasingly hydrophobic formulations using a twin screw granulator. International journal of
516 pharmaceutics 475, 82-96.

517

518

519 Figure 1.

520

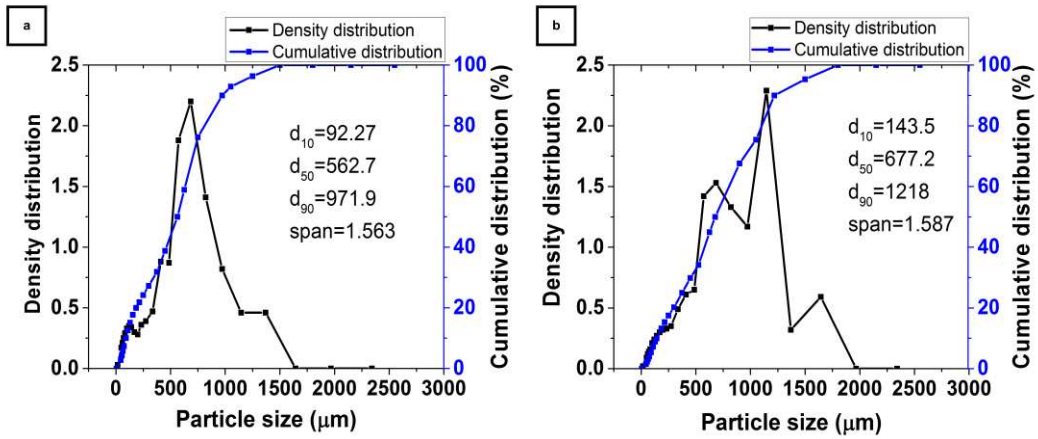

521

522 Figure 2.

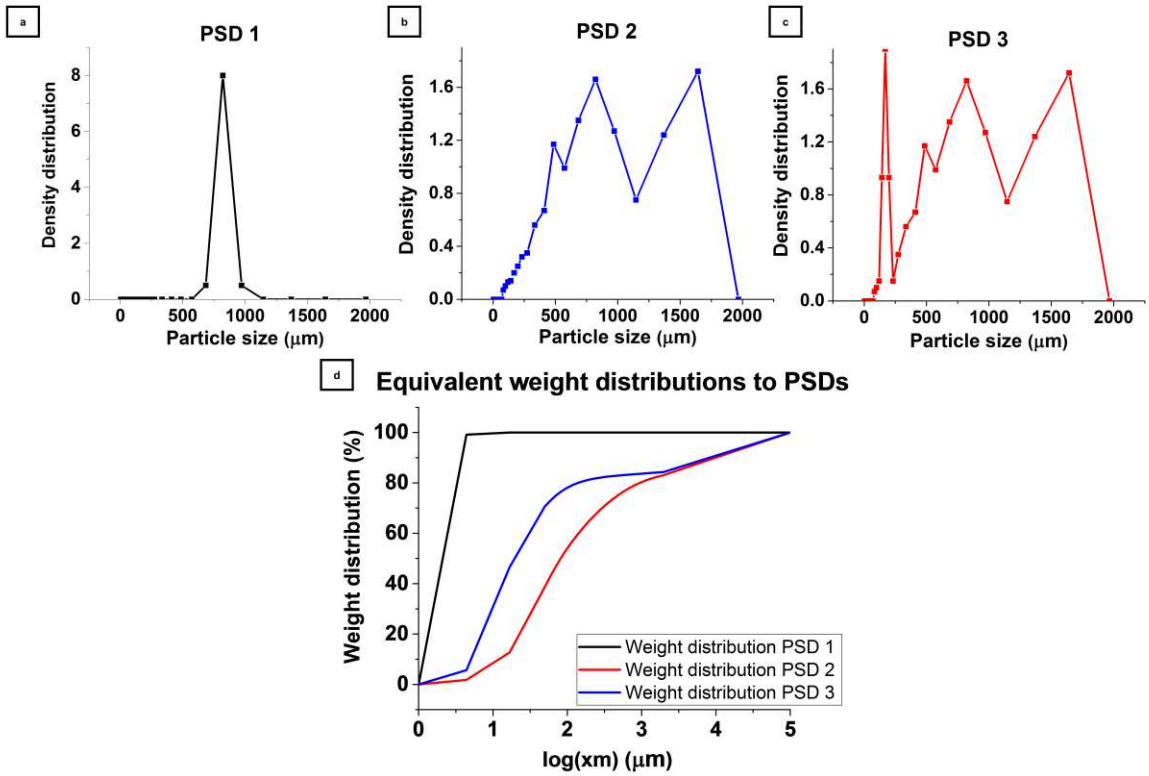

523

524

525 Figure 3.

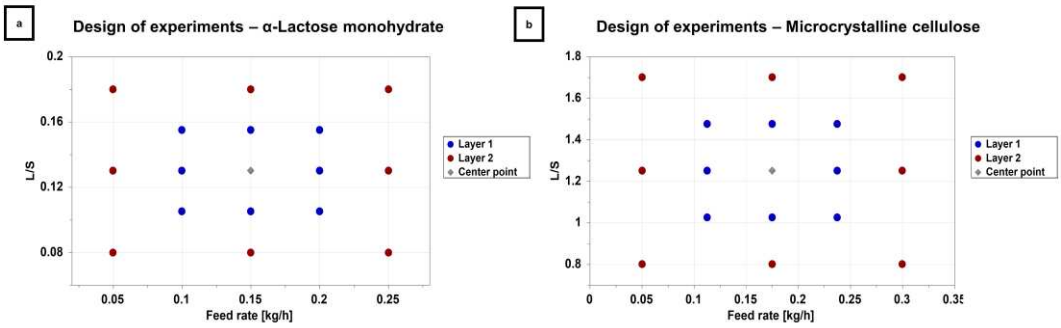

526

527

528 Figure 4.

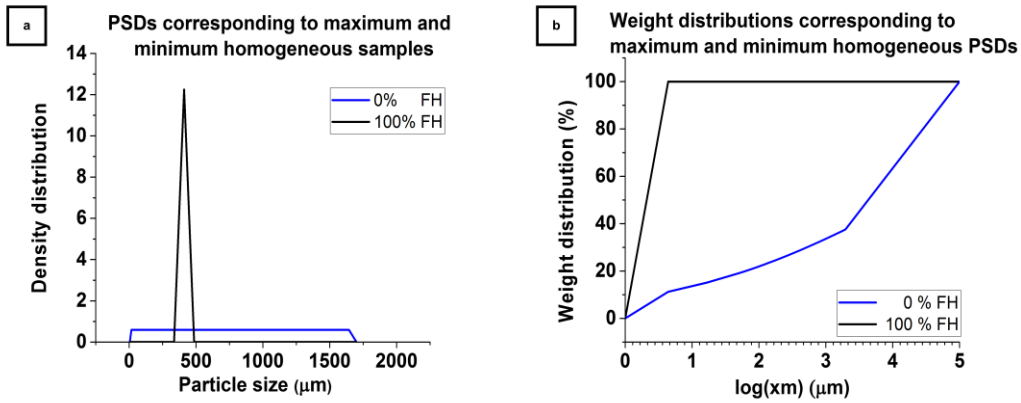

529

530

531 Figure 5.

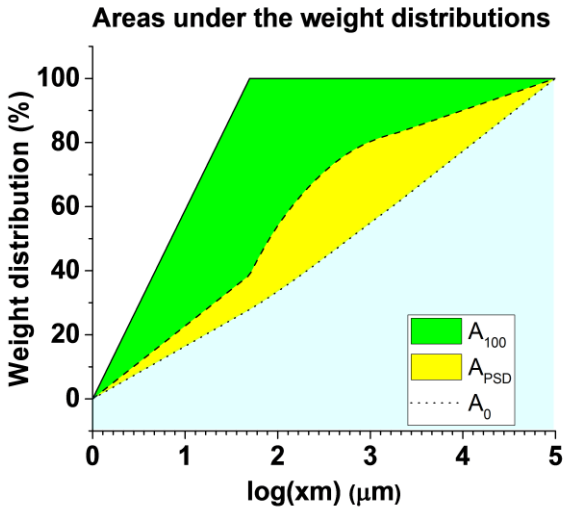

532

533

534 Figure 6.

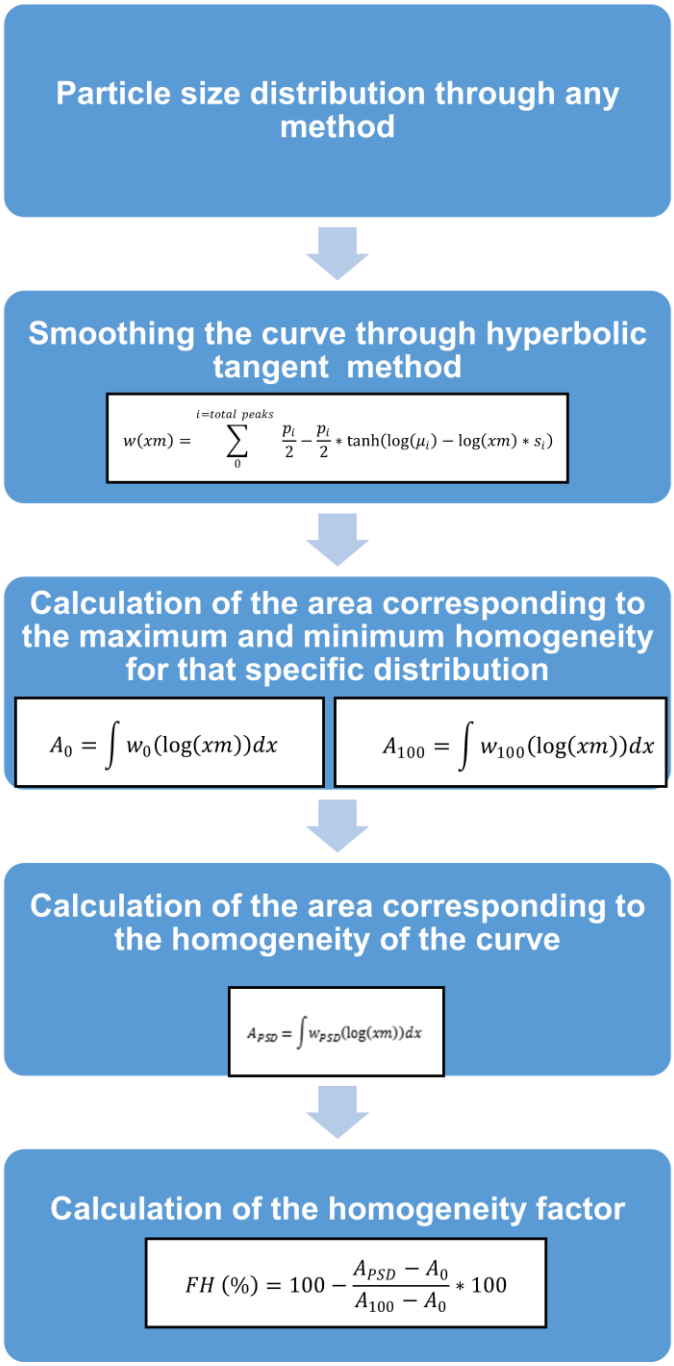

535

536

537 Figure 7.

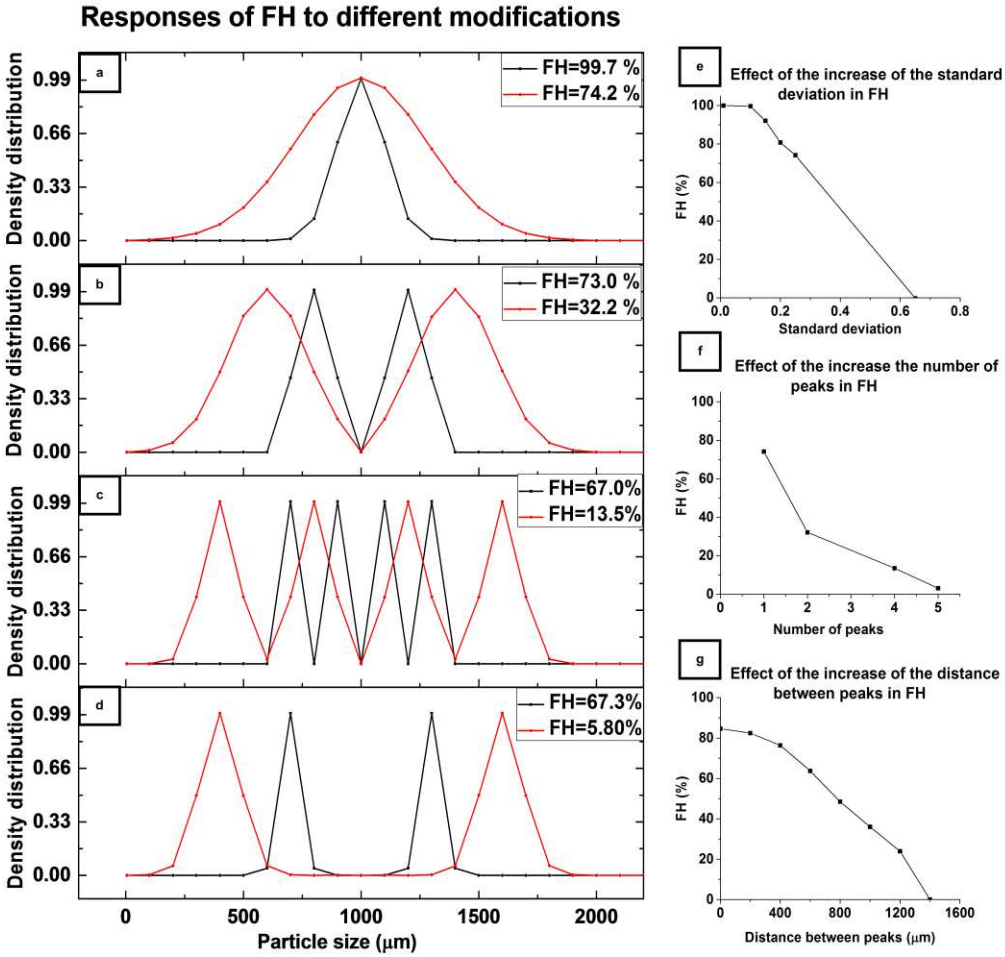

538

539

540 Figure 8.

541

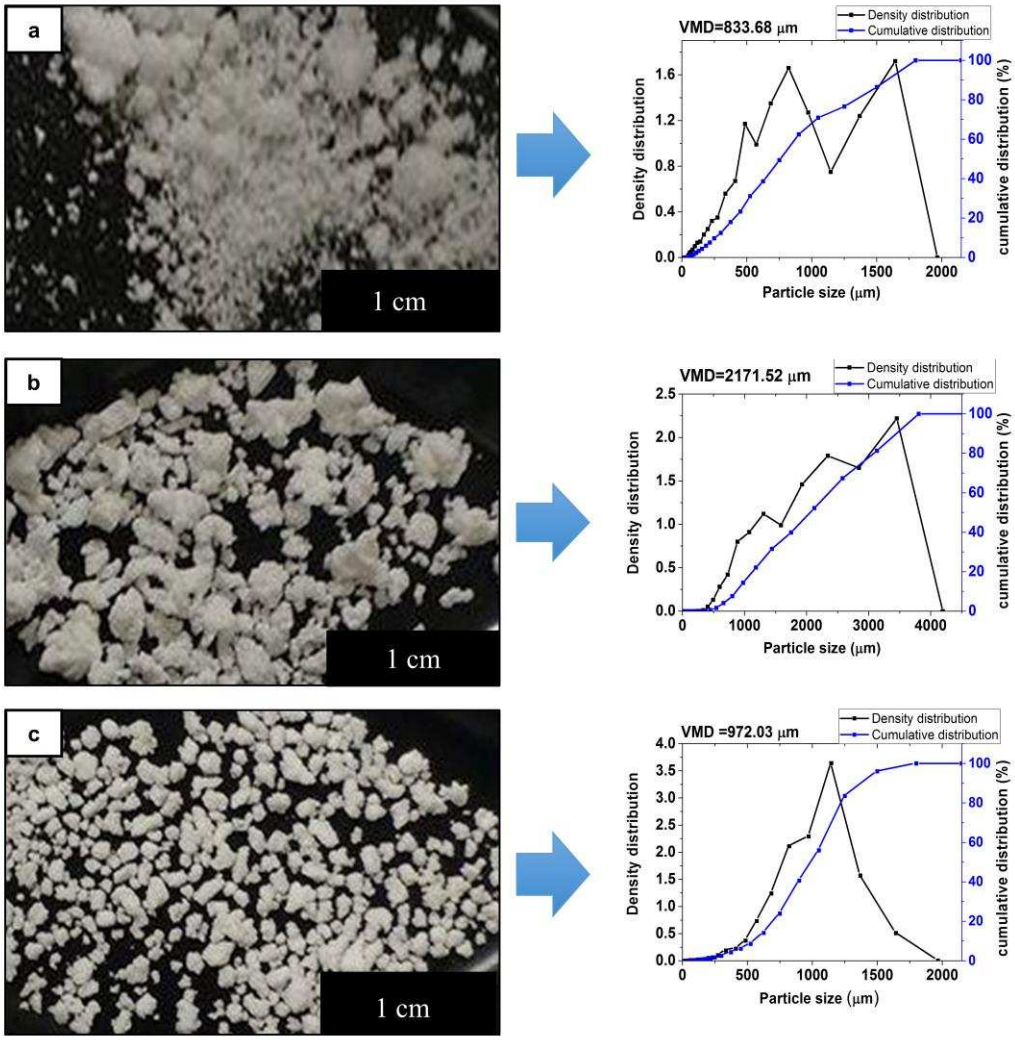

542

543 Figure 9.

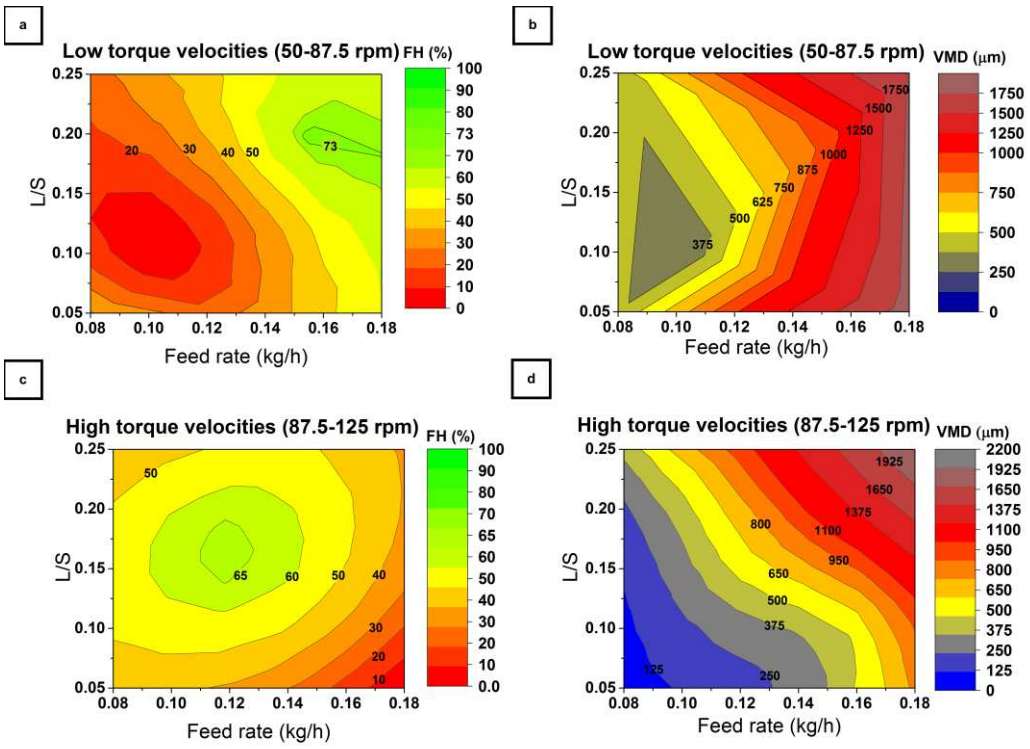

544

545

546 Figure 10.

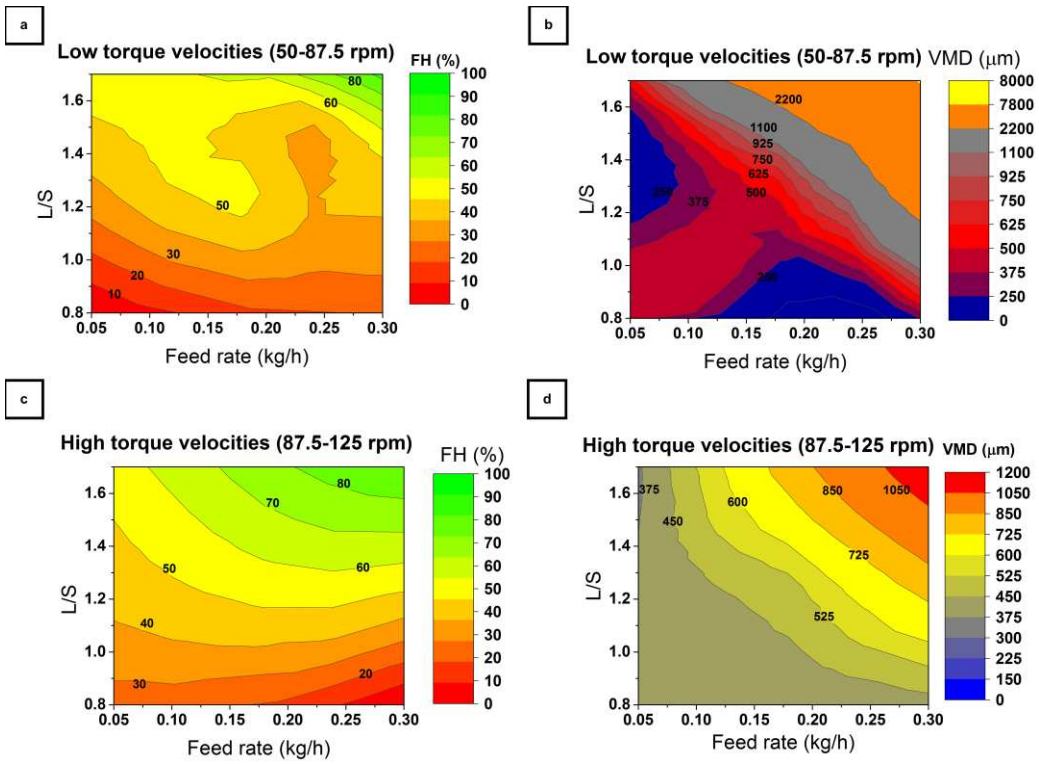

547

548